

Active Tectonics of the Garsela Fault Utilizing Morphotectonics and Seismicity in Garut Regency, Indonesia

Rafa Nurul Zahra Pristiwantoro¹, Fahrudin^{1,*}, Dian Agus Widiarso¹, Rio Alcanadre Tanjung Moechtar², Akbar Cita²

¹ Departement of Geological Engineering, Faculty of Engineering, Diponegoro University, Semarang, Central Java, Indonesia.

² Geological Survey Center, Geology Agency, Citarum, Bandung Wetan, Bandung, West Java, Indonesia.

* Corresponding author : fahrudin@ft.undip.ac.id

Tel.: +62-81-221-000-570;

Received: Dec 12, 2024; Accepted: May 31, 2025.

DOI: 10.24273/jgeet.2016.1.2.001

Abstract

Tectonic activity along active faults in Indonesia has a high potential to cause earthquakes with magnitudes greater than 6.5. This research focuses on the Garsela Fault in Garut Regency, West Java, which has a history of shallow earthquakes occurring near nationally important infrastructure. Morphotectonic analysis, Maximum Credible Earthquake (MCE) calculations, geological structure measurements, and subsurface condition assessments were conducted to determine the tectonic activity around the Garsela Fault and its fault mechanism. The analysis results show that tectonic activity in Garut Regency ranges from low to high. The Garsela Fault is divided into two segments with different fault systems: the Rakutai Segment, a normal fault (16.22 km), and the Kencana Segment, a strike-slip fault (17.33 km). MCE calculations for the Garsela Fault indicate potential maximum magnitudes of 5.42, 5.54, 6.28, and 6.54. Shallow earthquakes may produce stronger tremors in the western part of the Rakutai Segment compared to the east. In addition, earthquakes originating from the Kencana Segment may also generate tremors in the southern part of Garut Regency.

Keywords: Active Fault, Garsela Fault, Earthquake, Garut Regency

1. Introduction

Active faults are faults with displacements that occurred during the Quaternary period (Late Pleistocene and Holocene) and are expected to continue moving in the future (Trifonov and Kozhurin, 2010). On the island of Java, Indonesia, 34 active faults have been identified, all of which have the potential to generate intraplate earthquakes with magnitudes greater than 6.5 (Daryono et al., 2019; Lestari et al., 2020; Marliyani et al., 2016; Tim Pusat Studi Gempa Nasional, 2017; Adhitama, 2020; Ekarsti et al., 2023; Librian et al., 2024). One example of an active fault is the Garsela Fault, located in Garut Regency, West Java (Supendi et al., 2018). The fault is situated in the South Garut Zone and extends in a northeast-southwest direction from South Garut to South Bandung. It consists of two segments: the Kencana Segment in the southwest and the Rakutai Segment in the northeast, both of which have experienced several historical shallow earthquakes of relatively small magnitudes (Figure 1) (Arisbaya et al., 2021).

The surface geology in the South Garut Zone is dominated by young volcanic material that tends to be unconsolidated (Figure 1, conical mountain units), making the area susceptible to small-magnitude earthquakes. Earthquakes originating from the Garsela Fault have the potential to produce significant ground shaking. Several nationally important infrastructure facilities are located near the earthquake source, including geothermal power plants (PLTP) and hydroelectric power plants (PLTA), namely PLTP Wayang Windu, Darajat, Kamojang, and PLTA Lamajang. Disruption to these critical facilities could

potentially affect the stability of electricity supply for both local communities and the national industrial sector (Arisbaya et al., 2021).

This research aims to analyze the active tectonics and maximum earthquake potential of the Garsela Fault. The results can serve as a reference for spatial planning and infrastructure development, as well as inform earthquake disaster mitigation efforts in Garut Regency.

2. Methods

This research was conducted in Garut Regency, West Java, with a focus on the potential earthquake magnitudes that could be generated by the Garsela Fault. The study employed several methods, including morphotectonic analysis, structural kinematics analysis, and earthquake magnitude analysis. The maximum potential earthquake magnitude was calculated using the Maximum Credible Earthquake (MCE) method.

This study employed morphotectonic analysis (Doornkamp, 1986; Keller and Pinter Nicholas, 1996; Jannah et al., 2024; Martono et al., 2022), utilizing three parameters: the Basin Shape Index (Bs), Drainage Density (Dd), and Mountain Front Sinuosity (Smf). The classification criteria for each parameter are as follows:

Table 1. Classification of Values for Parameter Bs

Bs Values	Class
> 4	Class 1 (High Tectonic)
3 < Bs < 4	Class 2 (Moderate Tectonic)
< 3	Class 3 (Low Tectonic)

Table 2. Classification of Values for Parameter Dd

Dd Values	Class
5.5 < Dd < 8.2	Class 1 (High Tectonic)
4.14 < Dd < 5.5	Class 2 (Moderate Tectonic)
Dd < 4.14	Class 3 (Low Tectonic)

Table 3. Classification of Values for Parameter Smf

Smf Values	Class
< 1.1	Class 1 (High Tectonic)
1.1 < Smf < 1.5	Class 2 (Moderate Tectonic)
> 1.5	Class 3 (Low Tectonic)

The assessment of tectonic activity using the Basin Shape Index (Bs) interprets elongate sub-watersheds as indicative of high tectonic activity, classified as Class 1. For the Drainage Density (Dd) parameter, denser drainage patterns are associated with higher tectonic activity. The Mountain Front Sinuosity (Smf) parameter indicates that relatively straight mountain fronts correspond to high tectonic activity. Conversely, lower values or less pronounced characteristics in these parameters correspond to lower level of tectonic activity (Doornkamp, 1986; Keller and Pinter Nicholas, 1996).

The class values from these three parameters (Bs, Dd, and Smf) are then averaged to calculate the Index of Relative Tectonic Activity (IATR). The IATR is computed using the formula: $IATR = (Bs \text{ value} + Dd \text{ value} + Smf \text{ value}) / \text{the number of parameters used}$. The resulting IATR value is then categorized into four classes based on the level of tectonic activity as follows:

- Class 1 (IATR = 1 - 1.5) - Very High Tectonic Activity
- Class 2 (IATR = 1.5 - 2) - High Tectonic Activity
- Class 3 (IATR = 2 - 2.5) - Moderate Tectonic Activity
- Class 4 (IATR = > 2.5) - Low Tectonic Activity

The kinematic analysis of the fault was conducted by processing data from joints associated with the Garsela Fault. These fractures were measured during field activities and then analyzed using stereographic projection. The results of the stereographic projection analysis were used to determine the type and direction of movement of the Garsela Fault.

The maximum magnitude potential of the Garsela Fault was calculated using the Maximum Credible Earthquake (MCE) method following fault type determination. The calculation employs the equation developed by Wells and Coppersmith, Kevin, (1994) which uses fault length as a parameter. The equation is as follows :

- Reverse/Thrust fault with $M_{max} = 5.00 + 1.22 \times \log_{10}(\text{length of fault})$ (1)
- Strike Slip Fault with $M_{max} = 5.16 + 1.12 \times \log_{10}(\text{length of fault})$ (2)
- Normal Fault with $M_{max} = 4.86 + 1.32 \times \log_{10}(\text{length of fault})$ (3)

3. Geology Regional

The research area is located in Garut Regency, which is part of the Southern Mountains physiographic zone of West Java and is partially within the Quaternary Volcano zone. The region's morphology consists of conical mountains and high hills, as depicted in the West Java-Banten Morphological Unit Map (Ipranta et al., 2010) (Figure 1). Several active volcanoes surround Garut Regency, including Papandayan, Guntur, and Galunggung, along with several inactive mountains (Supendi et al., 2018).

The research area is generally composed of Quaternary volcanic rocks in the north and Tertiary volcanic rocks in the south, with weathered volcanic rocks present in some locations (Silitonga, 1973; Koesmono et al., 1996; Alzwar et al., 1992). The volcanic rocks were formed as a result of volcanic eruptions that released lava, volcanic ash, and other pyroclastic materials. Tertiary volcanic rocks consist of andesite, andesite breccia, volcanic breccia, lapilli tuff, dacite, and are related to diorite intrusions (Oo et al., 2019). Meanwhile, in some areas of Garut, especially in river valleys and lowland areas, there are sedimentary rock deposits in the form of alluvial deposits.

The geological structures observed in the area include folds, faults, and joints. The folds exhibit NWW-SEE axis directions in the Bentang Formation and NNW-SSE directions in the Jampang Formation (Alzwar et al., 1992). Joint structures are found in the Jampang Formation and quartz diorite. The faults consist of normal faults and strike-slip faults with NE-SW orientations. These faults cut through both Tertiary and Quaternary rocks, indicating the presence of both older and younger fault systems in Garut Regency (Haryanto, 2006; Hilmi and Haryanto, 2008).

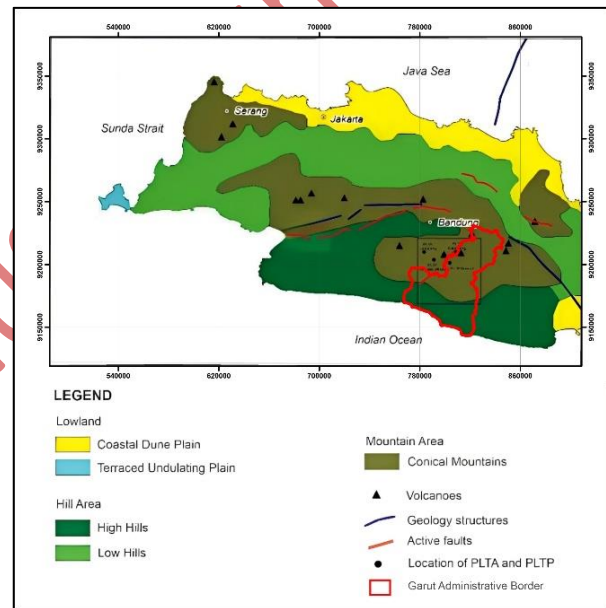


Fig 1. Map of Morphological Units of Banten and West Java with additional Active Faults (Ipranta et al., 2010)

4. Results

4.1 Regional Seismicity

The West Java is located in a seismically active zone, with earthquake sources originating from tectonic plate movements associated with the Java-Sumatra subduction zone and active fault systems (Kertapati et al., 2001). The distribution of earthquake epicenters in the West Java, particularly around Garut Regency, based on BMKG data from 2009 to 2022, shows that most events are shallow (depths ≤ 10 km) with magnitudes ranging from 1 to 4 (Table 4). This pattern provides evidence of recurring seismic activity in the region up to the present day. The ongoing tectonic activity in Garut Regency, as indicated by these inland earthquakes, is likely associated with the Garsela Fault.

Table 4. Some Seismicity Data of Earthquakes in Garut Regency and surrounding areas in 2009-2022 with depth ≤ 10 km

No	Time	Longitude	Latitude	Depth (Km)	Magnitude
1	07/13/2010	107.6115	-7.2063	5.661	2.8
2	02/29/2012	107.6609	-7.1441	2.621	3.2
3	6/5/2013	107.6916	-7.2938	4.091	3.1
4	01/27/2014	107.3296	-7.1323	9.042	3.2
5	05/26/2015	107.7151	-7.2073	8.612	3.3
6	02/23/2016	107.6671	-7.2127	2.175	2.3
7	9/7/2018	107.6375	-7.2392	0.432	2.6
8	4/6/2019	107.5885	-7.1601	5.433	2.4
9	11/28/2020	107.491798	-7.157878	4.384	2.6
10	08/29/2021	107.5806	-7.2134	9.2	2
11	8/3/2022	107.409996	-7.116305	10	2.8

Based on the seismicity pattern (Figure 2a, c), the study area is divided into two zones with significant shallow earthquake activity: The Samarang-Leles-Tarogong zone and The Talegong-Cisewu-Bungbulang-Cikelet zone.

A vertical cross-section (B-B') was created for these zones, revealing several inferred faults in both areas, most of which have predominantly northwest-dipping orientations (Figure 2b).

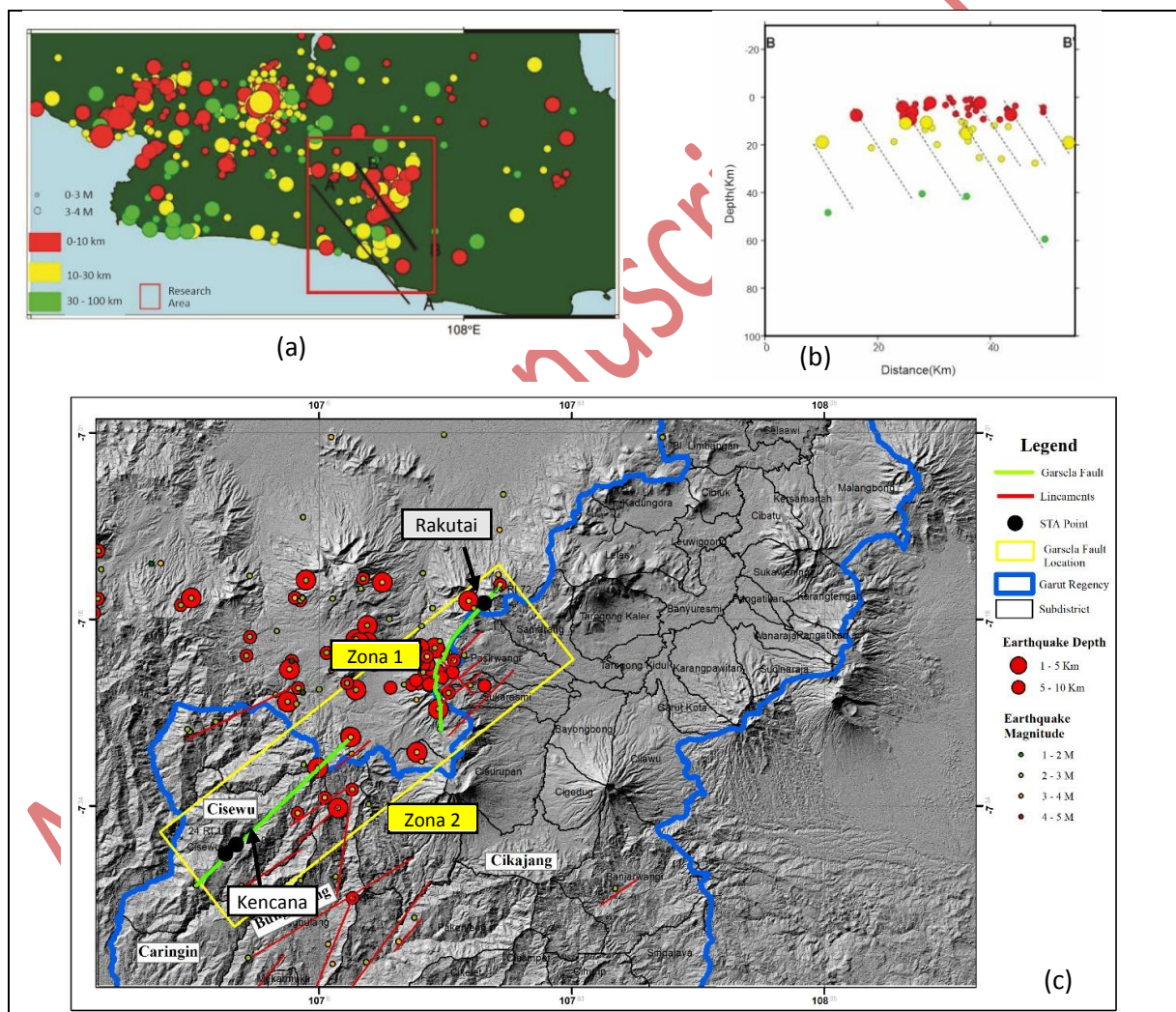


Fig 2. Regional seismicity with varying earthquake depths seen in cross section (a, b). The condition of the Rakutai Segment (north) Kencana Segment (south) of the Garsel Fault, and the seismicity distribution of shallow earthquakes (<10 km) (c) (modified from Moechtar et al., 2024)

4.2 Morphotectonic Analysis

The morphotectonic analysis using three parameters (Dd, Bs, and Smf) produced in Index of Relative Tectonic Activity (IATR) values for 414 sub-basins, which were

categorized into four classes: Very High, High, Moderate, and Low Tectonic Activity (Figure 3d). In Garut Regency, a straight line (shown in red in Figure 3) represents the Garsela Fault, which is divided into the Rakutai and Kencana segments by a dashed black line. The levels of

tectonic activity are classified as follows: class 4 (Low Tectonic Activity), class 3 (Moderate Tectonic Activity), and class 2 (High Tectonic Activity).

The sub-watershed shape (Bs) and drainage density (Dd) values predominantly indicate class 1 tectonic activity east of the Garsela Fault (Rakutai segment), while in the Kencana segment, both parameters are evenly distributed around the fault (Figures 3a, 3b). The Mountain Front Sinuosity (Smf) parameter, with low values indicating high

tectonic activity, is observed only around the Rakutai segment of the Garsela Fault (Figure 3c). The differing tectonic classifications of the two segments suggest distinct fault geometries. In the Rakutai segment, the class 1 tectonically active area indicates a region experiencing uplift, while the western side undergoes subsidence. In contrast, both blocks in the Kencana segment experience uplift.

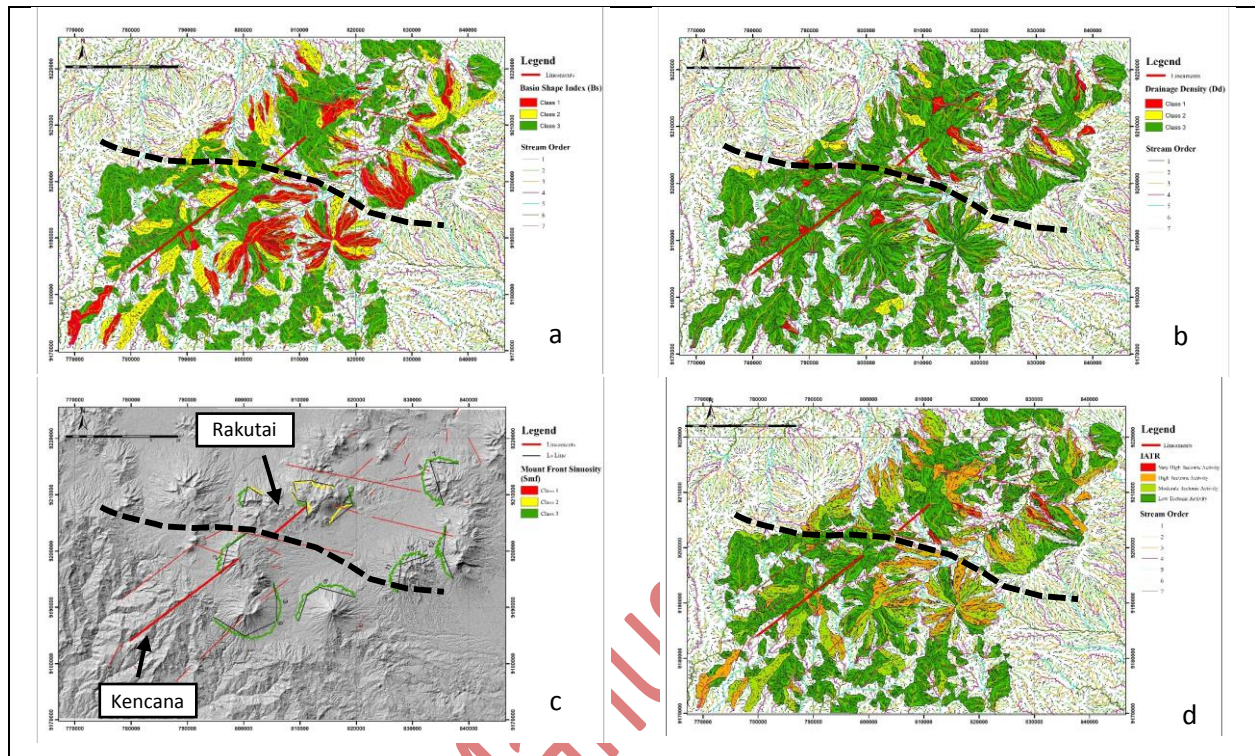


Fig 3. View of three maps of active tectonic parameters (a, b, c) and Index of Relative Tectonic Activity (IATR) map in Garut Regency and surrounding areas (d). The dashed back line is the boundary of Rakutai and Kencana segments.

4.3 Kinematics Analysis of Fault and Associated Structures

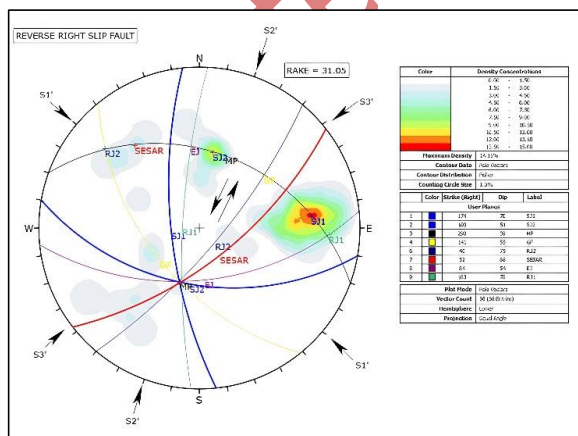


Fig 4. Data Processing Results STA 24 RI 01

The fault kinematics analysis utilizes joint orientation data collected from three distinct STA locations: STA 24 RI 01 at Rahong Waterfall, STA 24 RI 107 at Dengdeng Waterfall, and STA 24 RI 72 at Lake Ciharus. STA 24 RI 72 represents the Rakutai Segment (North), while STA 24 RI 01 and STA 24 RI 107 represent the Kencana Segment (South)

of the Garsela Fault, as illustrated in Figure 3. This analysis is similar to that conducted by Syahputra et al., (2019) in Belik Distric, Central Java.

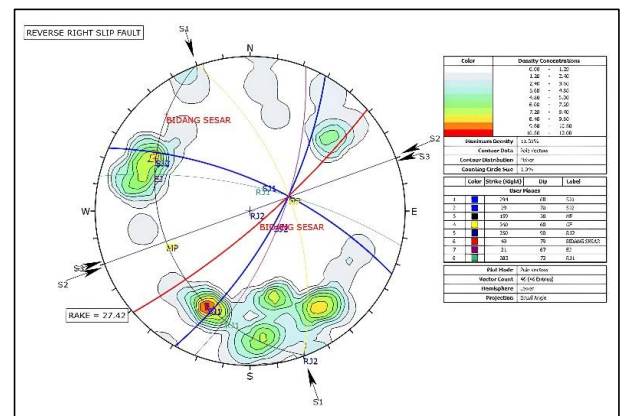


Fig 5. Data Processing Results STA 24 RI 107

The analysis results reveal distinct fault types at each STA location. STA 24 RI 01 exhibits a sinistral strike-slip fault type, as shown in Figure 4. STA 24 RI 107 displays a normal oblique-slip fault type, as presented in Figure 5. STA 24 RI 72 demonstrates a sinistral strike-slip fault type.

However, Supendi et al., (2018) argued that the Rakutai segment exhibited normal slip motion, while the Kencana segment shows strike-slip movement, based on P and S wave arrival time analysis of the November 6, 2016, and July 18, 2017 earthquakes. Furthermore, Arisbaya et al., (2021) proposed that the NE-SW trending structure (i.e., the Garsela Fault) is a strike-slip fault reactivated as a normal fault.

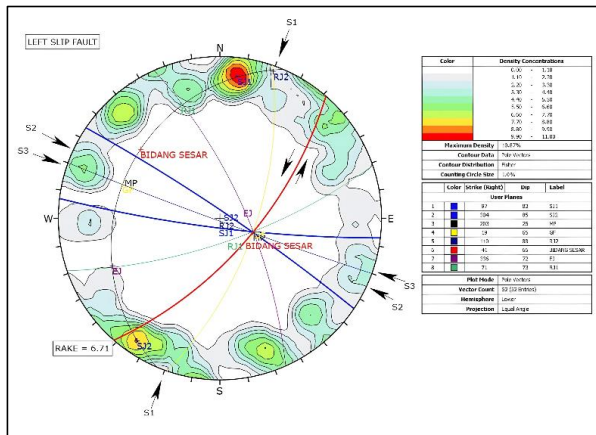


Fig 6. Data Processing Results STA 24 RI 72

Both earthquakes caused significant ground displacement in the southern part of Garut, specifically in

Tjitalahab, Ciawi, Cikajang, Awilaga, and Pameungpeuk, with shifts ranging from 1.5 to 3.4 cm according to InSAR analysis (Moechtar et al., 2024). This displacement is located near the Kencana segment of the Garsela Fault.

4.4 Calculation of the Maximum Potential Earthquake Magnitude for the Garsela Fault

The analysis of fault kinematics and associated structures at STA 24 RI 01 and STA 24 RI indicates that the Garsela Fault consists of a sinistral strike-slip in the northern Rakutai segment and a sinistral strike-slip slip fault in the southern Kencana segment. Consequently, the Garsela Fault is classified as a strike-slip fault.

Based on this classification, the equation used for magnitude calculation is:

$$M_{max} = 5.16 + 1.12 \times \log_{10}(\text{length of fault}).$$

The fault length of each segment is as follows:

- Rakutai Segment (north): 16.22 km (comprising four sub-segments).
- Kencana Segment (south): 17.33 km.

These lengths were determined through straight-line mapping on remote sensing images and aerial photographs, supplemented by previous study (Rejeki et al., 2010; Winarto et al., 2019). The calculation results are presented in Table 5 below.

Table 5. Calculation results of Maximum Potential Earthquake Magnitude on the Garsela Fault

No	Structure	Segment	Location				Province	City	Type of Structure		Length (Km)	Mag M_{max1}
			Geographic System		Type	Strike			Dip			
Lat 1	Long 1	Lat 2	Long 2									
1	Sesar Garsela	Rakutai - Sub 1	7° 12.734' S	107° 42.903' E	7° 8.628' S	107° 46.140' E	West Java	Garut Regency	Strike-slip fault		10.057	6.28
2	Sesar Garsela	Rakutai - Sub 2	7° 12.694' S	107° 42.852' E	7° 13.760' S	107° 42.434' E	West Java	Garut Regency	Strike-slip fault	41 66	2.212	5.54
3	Sesar Garsela	Rakutai - Sub 3	7° 13.797' S	107° 42.507' E	7° 14.934' S	107° 42.656' E	West Java	Garut Regency	Strike-slip fault		2.220	5.54
4	Sesar Garsela	Rakutai - Sub 4	7° 15.925' S	107° 42.875' E	7° 15.008' S	107° 42.677' E	West Java	Garut Regency	Strike-slip fault		1.731	5.42
5	Sesar Garsela	Kencana / Selatan	7° 22.770' S	107° 31.405' E	7° 17.355' S	107° 38.844' E	West Java	Garut Regency	Strike-slip fault	52 66	17.334	6.54

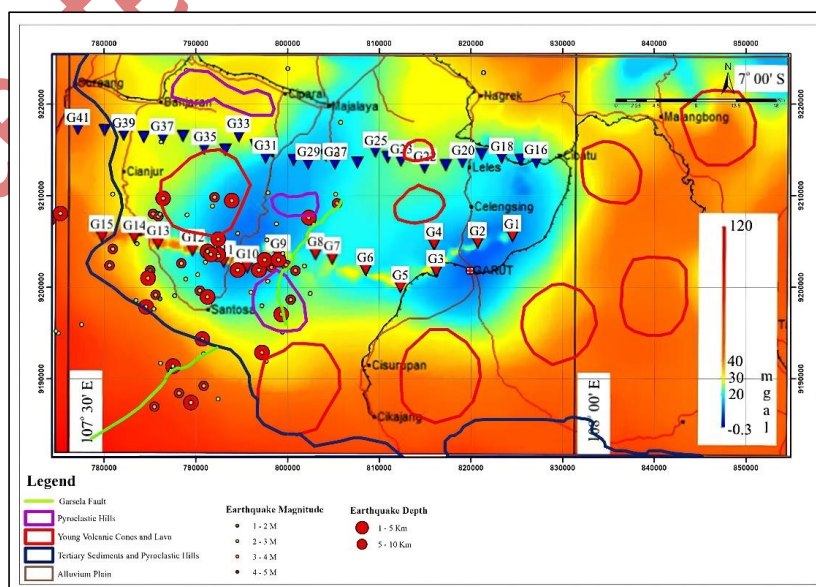


Fig 7. Gravity values and magnetotelluric section intersecting the Rakutai segment of the Garsela fault (north) are associated with the volcanic cone morphology widely distributed east of the Garsela Fault (modified from Handayani et al., 2013).

5. Discussion

5.1 Active tectonic and seismicity related to Garsela Fault

The seismicity shown in Figure 2a and 2b indicates that both deep and shallow earthquakes exhibit slope-aligned pattern (dashed line). This slope may correspond to the inclination of the earthquake amplification propagation zone. The dip direction aligns with the magnetotelluric data interpretation of the Garsela segment of the Rakutai Fault, which show a southwestward orientation (Handayani et al., 2013; Moechtar et al., 2024) (Figures 7 and 8).

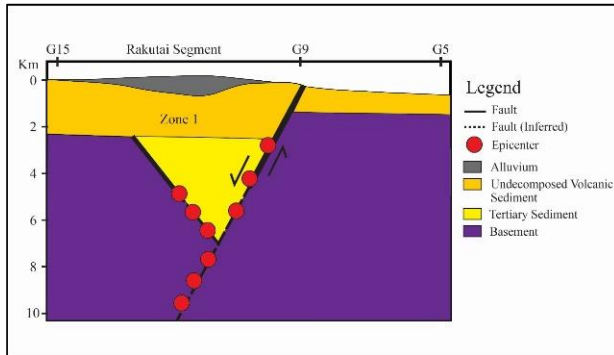


Figure 8. Illustration of the Rakutai segment of the Garsela fault, a normal fault as a source of shallow earthquakes (modified from Handayani et al., 2013; Moechtar et al., 2024)

Fahrudin et al., (2022) and Hendriyana and Tsuji, (2021) noted that shallow tremors accumulation is controlled by the shear zone (low-velocity zone), leading to steeper seabed elevation gradients in high tremor areas. Additionally, morphotectonic studies of Cilaki region in southern Garut demonstrate active tectonic influences on landforms and drainage systems, as evidenced by parameters such as Bs, Dd, Smf, Vf ratio, and Rc (Winarto et al., 2019). However, the morphotectonics around the Garsela Fault yield high IATR values indicative of active tectonics (i.e., Bs and Dd class 1 values; Figure 3), no shallow earthquakes accumulation is observed east of the Rakutai segment. This eastern area is uplifted due to the footwall block of the normal fault (Arisbaya et al., 2021; Supendi et al., 2018). In contrast, shallow earthquakes clusters are concentrated in the Kencana segment block and west of the Rakutai segment (Figure 2c). This suggests that shallow earthquakes (1-10 km) are likely controlled by shear zones within the hanging wall of the Rakutai segment of the Garsela Fault.

5.2 Earthquake amplification influenced by fault geometry of Garsela

An overlay of morphotectonic aspects, seismicity data (depth of ≤ 10 km), gravity, and magnetotellurics shows that earthquake epicenters (magnitude 1-5) at depths of ≤ 10 km accumulate in areas with low gravity values (indicated by blue color, representing a basin) and high gravity values (indicated by red color, representing basement highs). Basins and basement structures represented the extensional process of crustal thinning, where overburden caused stress accumulation on faults, potentially leading to earthquakes (Fahrudin, Aribowo, 2024; Hanif M, Handayani L, Arisbaya I, Nur Aulia A, 2021). This distribution highlights the geometry of the Garsela Fault (Arisbaya et al., 2021; Handayani et al., 2013; Supendi et al., 2018; Tim Pusat Studi Gempa Nasional, 2017) related basement structures. These data reinterpret the Garsela Fault as a half-graben normal fault (Figure 8). Since earthquakes accumulation is observed west of the Rakutai Segment (Zone 1) and around the Kencana Segment

(Zone 2), these earthquakes may increase differential stress and strain rates (Roberts et al., 2024), resulting in an amplification effect (tremor) in both zones (Figure 2). Similar tremors could be generated by the Cimandiri or Lembang fault due to the stress drop (Daryono et al., 2019; Prasetyo et al., 2023; Supendi et al., 2023).

Tremor effects will be concentrated in the fault zone, where the calculated maximum potential earthquake magnitude on the Garsela Fault ranges from 5.4 to 6.5 M (Table 5). Therefore, the tremor effects caused by shallow earthquakes (1-10 km) in Garut Regency, particularly in the west (west of the Rakutai segment/Zone 1) and south (around the Kencana segment/Zone 2), may be stronger than those in the east (e.g., Garut City). Thus, mitigation efforts for shallow earthquakes need to be enhanced in both zones. Given that many shallow earthquakes occur at depths of less than 2 km around the Drajat geothermal power plant area, it is essential to follow up on the tremor effect calculations to support the mitigation of national infrastructure.

6. Conclusion

Garsela Fault in the South Garut Zone, Garut Regency, is classified as an active fault based on its seismicity history and morphotectonic analysis from the IATR map. The morphotectonic results indicate that areas surrounding the Garsela Fault exhibit varying levels of tectonic activity, ranging from low to high. The morphotectonic data, MCE calculations, geological structure measurements, and subsurface conditions assessment of the Rakutai segment and Kencana segment of the Garsela Fault reveal different fault types. The two segments are classified as normal and strike-slip faults, with lengths of 16.22 km for the Rakutai segment and 17.33 km for the Kencana segment. The maximum earthquake magnitudes that can result from the activity of the Garsela Fault, based on calculations using the MCE method, are 5.42 M, 5.54 M, and 6.28 M for the Rakutai segment, while for the Kencana segment, it is 6.54 M.

Acknowledgements

Thank you to the Geological Survey Center, Geological Agency of Indonesia, and University of Diponegoro for their support in preparing the data and providing funding.

References

- Adhitama, R., 2020. Paleostress analysis of Baribis Fault system-Brebes segment based on outcrop fault data. *J. Geosci. Eng. Energy* 1, 61–67. <https://doi.org/10.25105/jogee.v1i02.7680>
- Arisbaya, I., Lestiana, H., Mukti, M.M., Handayani, L., Grandis, H., Warsa, Sumintadireja, P., 2021. Garsela Fault and other NE-SW active faults along the southern part of Java Island. *IOP Conf. Ser. Earth Environ. Sci.* 789, 0–7. <https://doi.org/10.1088/1755-1315/789/1/012065>
- Daryono, M.R., Natawidjaja, D.H., Sapiie, B., Cummins, P., 2019. Earthquake Geology of the Lembang Fault, West Java, Indonesia. *Tectonophysics* 751, 180–191. <https://doi.org/10.1016/j.tecto.2018.12.014>
- Doornkamp, J.C., 1986. Geomorphological approaches to the study of neotectonics. *J. - Geol. Soc.* 143, 335–342. <https://doi.org/10.1144/gsjgs.143.2.0335>
- Ekarsti, A.K., Pramumijoyo, S., Marliyani, G.I., Setianto, A., DwikoritaKarnawati, 2023. Analyzing Recent Seismic Activity of the Opak Fault System in Central Java, Indonesia, From 2009 To 2021. *Int. J. GEOMATE* 25, 87–97. <https://doi.org/10.21660/2023.110.3959>

- Fahrudin, Aribowo, Y., 2024. Review : Geological Structure Impacts to Hydrocarbon Potential and Active Faults in the East Java Basin, Indonesia. *J. Geosci. Eng. Environ. Technol.* 9, 379–383. <https://doi.org/10.25299/jgeet.2024.9.3.16736>
- Fahrudin, Chhun, C., Tsuji, T., 2022. Influence of shear zone thickness and strike-slip faulting on tectonic tremor in the Nankai Trough, southwest Japan. *Tectonophysics* 838, 229519. <https://doi.org/10.1016/j.tecto.2022.229519>
- Handayani, L., Kamtono, K., Wardhana, D.D., 2013. Extensional Tectonic Regime of Garut Basin based on Magnetotelluric Analysis. *Indones. J. Geosci.* 8, 127–133. <https://doi.org/10.17014/ijog.v8i3.162>
- Hanif M, Handayani L, Arisbaya I, Nur Aulia A, L.G.K., 2021. Analysis of gravity anomaly decomposition and depth to basement, case study: Cenozoic Bogor Basin, Indonesia. *J. Geosci. Eng. Environ. Technol.* 6.
- Haryanto, I., 2006. Struktur Geologi Paleogen dan Neogen di Jawa Barat. *Bull. Sci. Contrib.* 4, 88–95.
- Hendriyana, A., Tsuji, T., 2021. Influence of structure and pore pressure of plate interface on tectonic tremor in the Nankai subduction zone, Japan. *Earth Planet. Sci. Lett.* 558, 116742. <https://doi.org/10.1016/j.epsl.2021.116742>
- Hilmi, F., Haryanto, I., 2008. Pola Struktur Regional. *Bull. Sci. Contrib.* 6, 57–66.
- Jannah, M., Pamumpuni, A., Sadisun, I.A., 2024. Segmentation of the Active Fault on the Cirebon-Semarang Segments as Revealed by DEM-Derived Geomorphic Indices. *J. Geosci. Eng. Environ. Technol.* 9, 385–399. <https://doi.org/10.25299/jgeet.2024.9.04.15572>
- Keller, E.A., Pinter Nicholas, 1996. *Active tectonics_Keller_Pinter_small*. Prentice hall.
- Lestari, W., Widodo, A., Syaifuddin, F., Warnana, D.D., 2020. Research priority of the potential earthquake on the java island using decision making analysis. *E3S Web Conf.* 156, 1–5. <https://doi.org/10.1051/e3sconf/202015603003>
- Librian, V., Ramdhan, M., Nugraha, A.D., Mukti, M.M., Syuhada, S., Lühr, B.G., Widiyantoro, S., Mursiantyo, A., Anggraini, A., Zulfakriza, Z., Muttaqy, F., Mi'rojul Husni, Y., 2024. Detailed seismic structure beneath the earthquake zone of Yogyakarta 2006 (Mw ~6.4), Indonesia, from local earthquake tomography. *Phys. Earth Planet. Inter.* 351, 107170. <https://doi.org/10.1016/j.pepi.2024.107170>
- Marliyani, G.I., Arrowsmith, J.R., Whipple, K.X., 2016. Characterization of slow slip rate faults in humid areas: Cimandiri fault zone, Indonesia. *J. Geophys. Res. Earth Surf.* 121, 2287–2308. <https://doi.org/10.1002/2016JF003846>
- Martono, Hasria, Asfar, S., Azzaman, M.A., Ngkoimani, L.O., Okto, A., Hamimu, L., Irawati, Sawaludin, Iradat Salihin, L.O.M., Wahab, 2022. Morphotectonic Control of Land Movements at Wundulako Region, Kolaka Regency, Southeast Sulawesi Province, Indonesia. *J. Geosci. Eng. Environ. Technol.* 7, 80–86. <https://doi.org/10.25299/jgeet.2022.7.2.9235>
- Moechtar, R., Wahyudiono, R., Rohman, Yuniarni, R., Sukapti, W., Yulianto, E., Sulandari, B., Lazari, O., Mutiah, S., 2024. Active Fault Map of Garut Regency, West Java. *ATLAS, Peta Temat. Patahan Aktif Kabupaten/Kota di Indones. Vo.*: 1.
- Oo, K.Y., Warmada, W., Titisari, A.D., Watanabe, K., 2019. Ore Forming Fluid of Epithermal Quartz Veins at Cisuru Prospect, Papandayan District, West Java, Indonesia. *J. Geosci. Eng. Environ. Technol.* 4, 170. <https://doi.org/10.25299/jgeet.2019.4.3.2279>
- Prasetio, R., Laksmingpuri, N., Satrio, S., Pujiindiyati, E.R., Pratikno, B., Sidauruk, P., 2023. The ²²²Rn and CO₂ soil gas distribution at Lembang Fault Zone, West Java - Indonesia. *J. Environ. Radioact.* 257, 107079. <https://doi.org/10.1016/j.jenvrad.2022.107079>
- Rejeki, S., Rohrs, D., Nordquist, G., Fitriyanto, A., 2010. Geologic Conceptual Model Update of the Darajat Geothermal Field, Indonesia. *Proc. World Geotherm. Congr.* 25–29.
- Roberts, G.P., Sgambato, C., Mildon, Z.K., Iezzi, F., Beck, J., Robertson, J., Papanikolaou, I., Michetti, A.M., Faure Walker, J.P., Meschis, M., Shanks, R., Phillips, R., McCaffrey, K.J.W., Vittori, E., Mitchell, S., 2024. Spatial migration of temporal earthquake clusters driven by the transfer of differential stress between neighbouring fault/shear-zone structures. *J. Struct. Geol.* 181, 105096. <https://doi.org/10.1016/j.jsg.2024.105096>
- Supendi, P., Nugraha, A.D., Puspito, N.T., Widiyantoro, S., Daryono, D., 2018. Identification of active faults in West Java, Indonesia, based on earthquake hypocenter determination, relocation, and focal mechanism analysis. *Geosci. Lett.* 5. <https://doi.org/10.1186/s40562-018-0130-y>
- Supendi, P., Winder, T., Rawlinson, N., Bacon, C.A., Palgunadi, K.H., Simanjuntak, A., Kurniawan, A., Widiyantoro, S., Nugraha, A.D., Shiddiqi, H.A., Ardianto, Daryono, Adi, S.P., Karnawati, D., Priyobudi, Marliyani, G.I., Imran, I., Jatnika, J., 2023. A conjugate fault revealed by the destructive Mw 5.6 (November 21, 2022) Cianjur earthquake, West Java, Indonesia. *J. Asian Earth Sci.* 257, 105830. <https://doi.org/10.1016/j.jseaes.2023.105830>
- Syahputra, R., Sihombing, F.M.H., Prasojo, O.A., 2019. Correlation Between Fracture Azimuth, Surface Lineaments and Regional Tectonics: A case study from Belik District, Central Java, Indonesia. *J. Geosci. Eng. Environ. Technol.* 4, 22. <https://doi.org/10.25299/jgeet.2019.4.1.2294>
- Tim Pusat Studi Gempa Nasional, 2017. *Peta Sumber dan Bahaya Gempa Indonesia Tahun 2017*. Pus. Litbang Perumahan dan Pemukiman, PU 376.
- Trifonov, V.G., Kozhurin, A.I., 2010. Study of active faults: Theoretical and applied implications. *Geotectonics* 44, 510–528. <https://doi.org/10.1134/S0016852110060051>
- Wells, D.L., Coppersmith, Kevin, J., 1994. New empirical relationship between magnitude, rupture length, rupture width, rupture area, and surface displacement. *Bull. Seismol. Soc. Am.* 84, 974–1002.
- Winarto, J., Sukiyah, E.M.I., Haryanto, A.D., Haryanto, I., 2019. Morphotectonic study of a watershed controlled by active fault in southern Garut, west Java, Indonesia. *J. Himal. Earth Sci.* 52, 96–105.



© 2025 Journal of Geoscience, Engineering, Environment and Technology. All rights reserved. This is an open access article distributed under the terms of the CC BY-SA License (<http://creativecommons.org/licenses/by-sa/4.0/>).